Wavelength Multistability in Lasers: The Effect of Spatial Hole Burning

Antonio Pérez-Serrano(1), Julien Javaloyes(2) and Salvador Balle(3)

(1) IFISC (UIB-CSIC), Palma de Mallorca, Spain
(2) Dept. of Electronics and Electrical Engineering, University of Glasgow, UK
(3) IMEDEA (UIB-CSIC), Esporles, Spain

IFISC

CSIC UIB

Outline

I. Motivation

II. The model

III. Longitudinal modal multistability in lasers:
Comparison between Ring and Fabry-Pérot configurations

IV. Conclusions

I. Motivation

- Ring Lasers can exhibit a rich variety of dynamical regimes:

Bidirectional CW
Alternate Oscillations
Modelocking
Bistability
Chaos
...

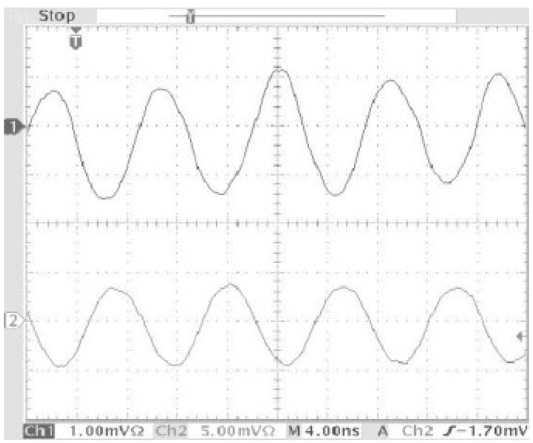

Sorel et al.
IEEE JQE **39**, 1187 (2003)

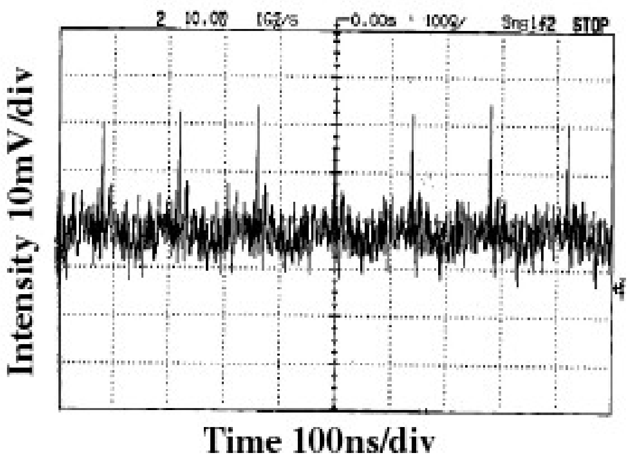

Zhang et al.
J. Opt. A. **7**, 175 (2005)

I. Motivation

- Ring Lasers can exhibit a rich variety of dynamical regimes:

Bidirectional CW
Alternate Oscillations
Modelocking
Bistability
Chaos
...

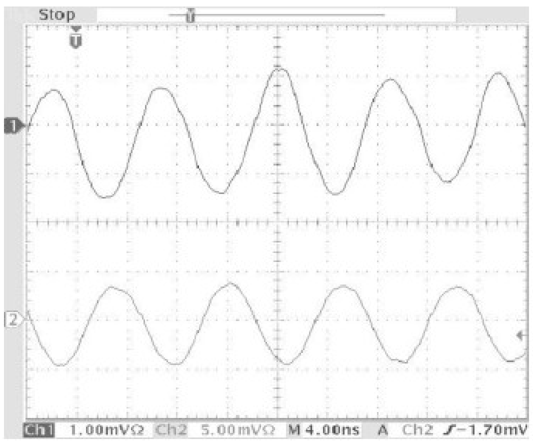

Sorel et al.
IEEE JQE **39**, 1187 (2003)

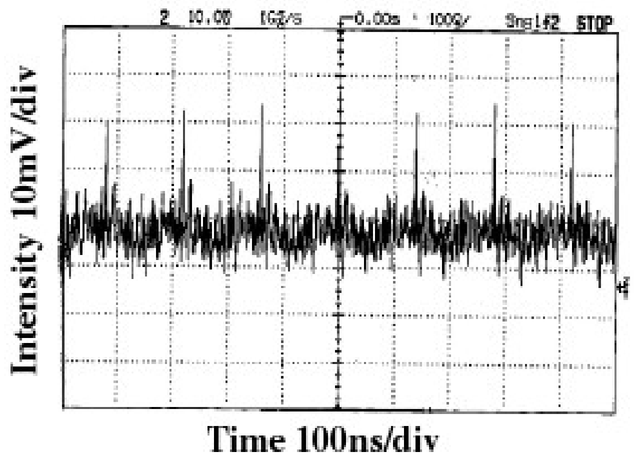

Zhang et al.
J. Opt. A. **7**, 175 (2005)

Bistability in directional emission ⟶ **All-optical binary logics**

Hill et al. Nature **432**, 206 (2004)

I. Motivation

- Experimental results show that in SRLs emission wavelength can be selected by optical injection, and the system remains stable at the chosen value.

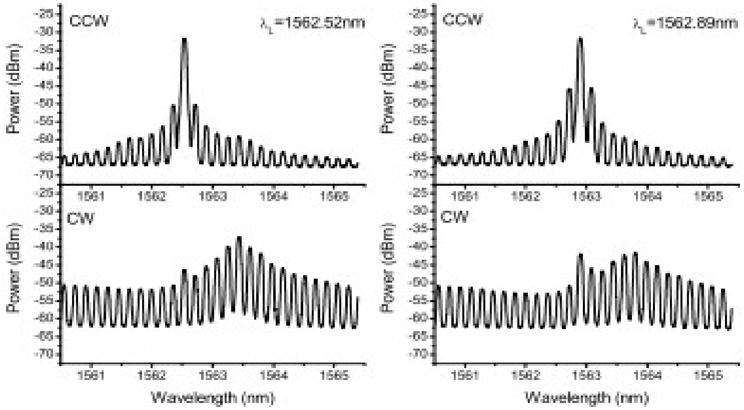

Born et al. IEEE JQE **41**, 261 (2005).

All-optical higher order logics

I. Motivation

- Experimental results show that in SRLs emission wavelength can be selected by optical injection, and the system remains stable at the chosen value.

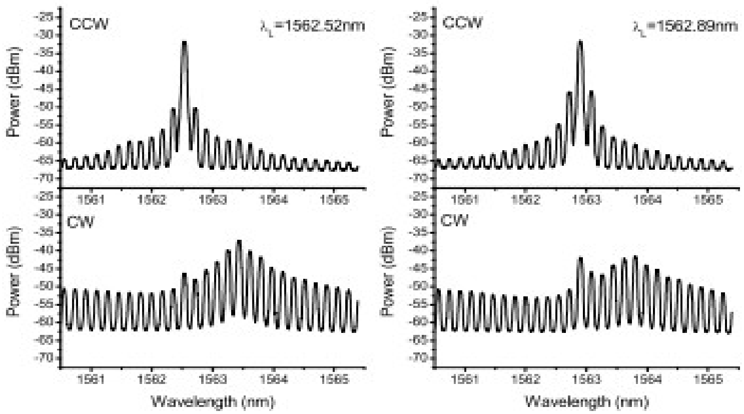

Born et al. IEEE JQE **41**, 261 (2005).

All-optical higher order logics

- Existing Models: Rate Equations-Like (ODEs)
Spatial dependence simplified

Modal couplings??

I. Motivation

- Experimental results show that in SRLs emission wavelength can be selected by optical injection, and the system remains stable at the chosen value.

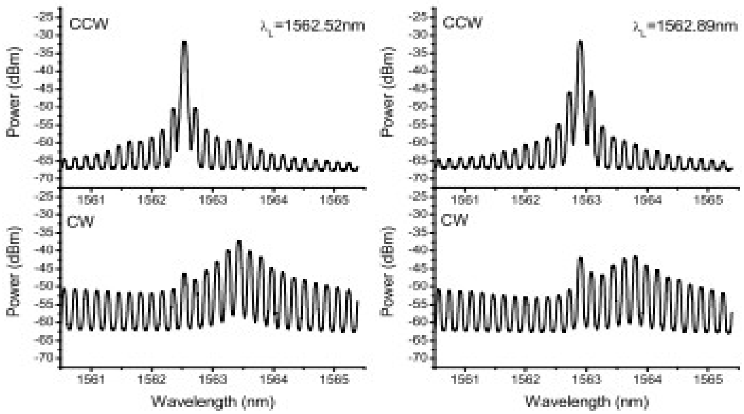

Born et al. IEEE JQE **41**, 261 (2005).

All-optical higher order logics

- Existing Models: Rate Equations-Like (ODEs)
  Spatial dependence simplified

Modal couplings??

- Comprehensive theory → Taking into account spatial effects / Modal couplings

- Generality of the TWM (PDEs): Description of different types of lasers.
  Multimode behavior arises naturally in a TWM description.

II. The model

Dimensionless TW Equations
for the SVA in a Semi-classical approach:

$$\pm\frac{\partial A_\pm}{\partial s}+\frac{\partial A_\pm}{\partial \tau}=B_\pm-\alpha A_\pm$$

Electric Fields

II. The model

Dimensionless TW Equations
for the SVA in a Semi-classical approach:

$$\pm\frac{\partial A_\pm}{\partial s}+\frac{\partial A_\pm}{\partial \tau}=B_\pm-\alpha A_\pm$$

Electric Fields

$$\frac{1}{\gamma}\frac{\partial B_\pm}{\partial \tau}=-(1+i\widetilde{\delta})B_\pm+g(D_0A_\pm+D_{\pm2}A_\mp)+\sqrt{\beta D_0}\xi_\pm(s,\tau)$$

Polarization

$$\frac{\partial D_0}{\partial \tau}=\epsilon[J-D_0+\Delta\frac{\partial^2 D_0}{\partial s^2}-(A_+B_+^*+A_-B_-^*+A_+^*B_++A_-^*B_-)]$$

$$\frac{\partial D_{\pm2}}{\partial \tau}=-\eta D_{\pm2}-\epsilon(A_\pm B_\mp^*+A_\mp^*B_\pm)$$

Carriers

IFISC

II. The model

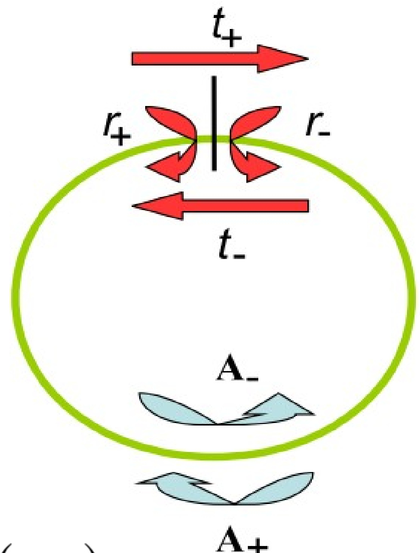

Dimensionless TW Equations
for the SVA in a Semi-classical approach:

$$\pm\frac{\partial A_\pm}{\partial s} + \frac{\partial A_\pm}{\partial \tau} = B_\pm - \alpha A_\pm$$

Electric Fields

$$\frac{1}{\gamma}\frac{\partial B_\pm}{\partial \tau} = -(1+i\tilde{\delta})B_\pm + g(D_0 A_\pm + D_{\pm 2} A_\mp) + \sqrt{\beta D_0}\,\xi_\pm(s,\tau)$$

Polarization

$$\frac{\partial D_0}{\partial \tau} = \epsilon\left[J - D_0 + \Delta\frac{\partial^2 D_0}{\partial s^2} - (A_+ B_+^* + A_- B_-^* + A_+^* B_+ + A_-^* B_-)\right]$$

$$\frac{\partial D_{\pm 2}}{\partial \tau} = -\eta D_{\pm 2} - \epsilon(A_\pm B_\mp^* + A_\mp^* B_\pm)$$

Carriers

Boundary Conditions:

$$A_+(0,\tau) = t_+ A_+(1,\tau) + r_- A_-(0,\tau)$$
$$A_-(1,\tau) = t_- A_-(0,\tau) + r_+ A_+(1,\tau)$$

FP : $t_\pm = 0$

Ideal Ring: $r_\pm = 0$

II. The model

Solving PDEs numerically:

Fleck, Phys. Rev. B **1**, 84 (1970).

Tests for the numerical algorithm:

Analytical Results (Unidirectional or UFL)

Zeghlache et al. Phys. Rev. A **37**, 470 (1988).

II. The model

Solving PDEs numerically:

Fleck, Phys. Rev. B **1**, 84 (1970).

Tests for the numerical algorithm:

Analytical Results (Unidirectional or UFL)

Zeghlache et al. Phys. Rev. A **37**, 470 (1988).

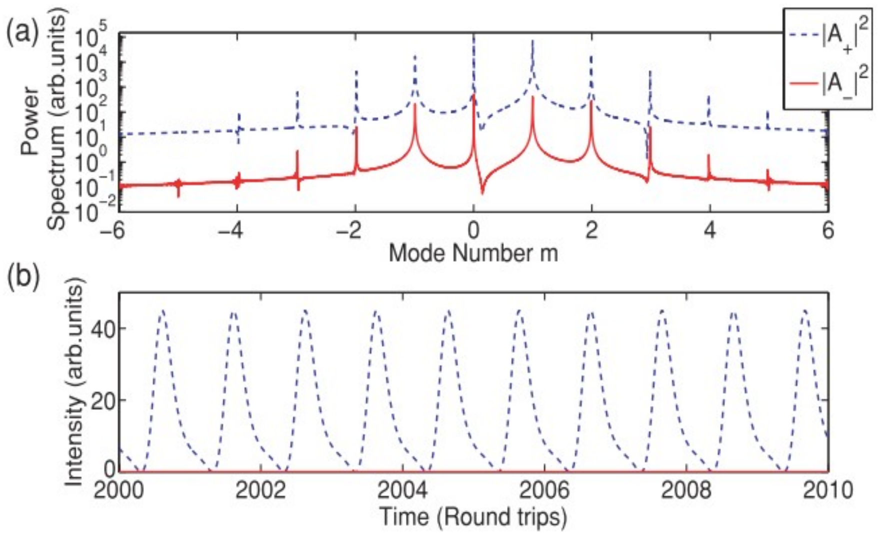

For details: Pérez-Serrano et al. Phys. Rev. A **81**, 043817 (2010).

II. The model

Solving PDEs numerically:

Fleck, Phys. Rev. B **1**, 84 (1970).

Tests for the numerical algorithm:

Analytical Results (Unidirectional or UFL)

Zeghlache et al. Phys. Rev. A **37**, 470 (1988).

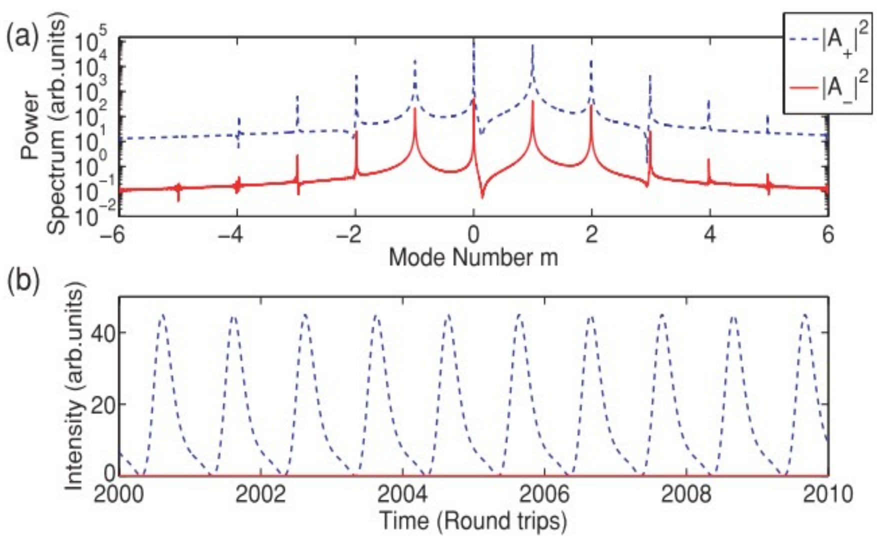

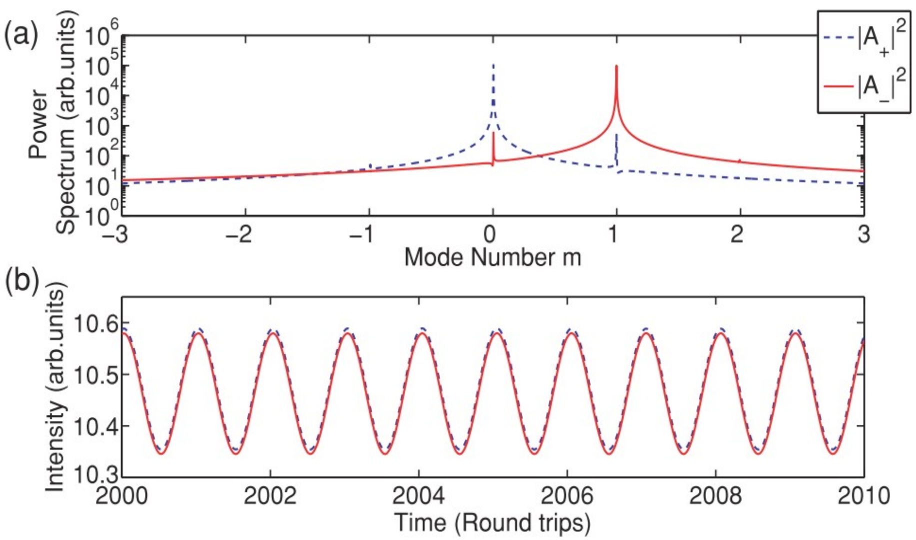

For details: Pérez-Serrano et al. Phys. Rev. A **81**, 043817 (2010).

III. Longitudinal modal multistability in lasers

Ascertaining multistability → Monochromatic solutions Eigenvalue problem → Analytically difficult in the general case

III. Longitudinal modal multistability in lasers

Ascertaining multistability → Monochromatic solutions Eigenvalue problem → Analytically difficult in the general case

- Monochromatic Solutions via a low dimensional shooting method.

→ Discretized representation of the modal profile.

III. Longitudinal modal multistability in lasers

Ascertaining multistability → Monochromatic solutions Eigenvalue problem → Analytically difficult in the general case

- Monochromatic Solutions via a low dimensional shooting method.
  → Discretized representation of the modal profile.

- Eigenvalue Problem:
  - Hyperbolic PDE: discrete representation of the gradient
  → Large error in the computed eigenvalues.

III. Longitudinal modal multistability in lasers

Ascertaining multistability → Monochromatic solutions Eigenvalue problem → Analytically difficult in the general case

- Monochromatic Solutions via a low dimensional shooting method.
  → Discretized representation of the modal profile.

- Eigenvalue Problem:
  - Hyperbolic PDE: discrete representation of the gradient
    → Large error in the computed eigenvalues.

  - Linearized evolution operator → Floquet multipliers

- This approach is quite general: can be used in other dynamical systems with PDEs.

III. Longitudinal modal multistability in lasers

Bidirectional Ring laser

LSA for mode m = 2

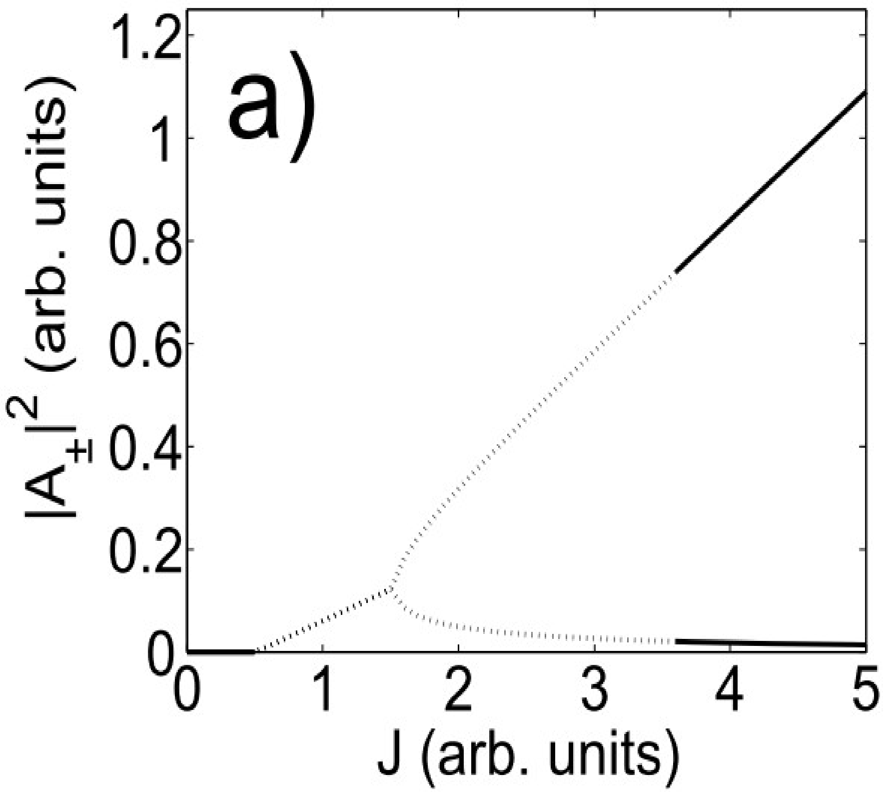

$g = 4$
$t_\pm = 0.98$
$r_\pm = 0.01$
$\varepsilon = 0.05$
$\eta = 10$
$\gamma = 250$
$\Delta = 0$
$\alpha = 2.03$

Typical parameters for semiconductor lasers

III. Longitudinal modal multistability in lasers

Bidirectional Ring laser

LSA for mode m = 2

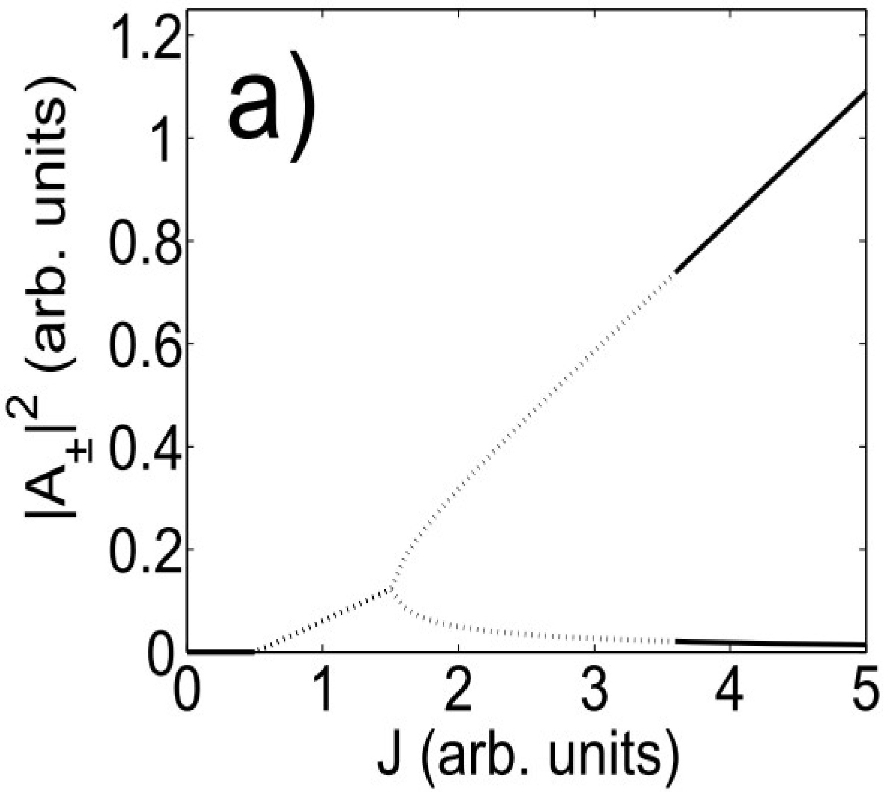

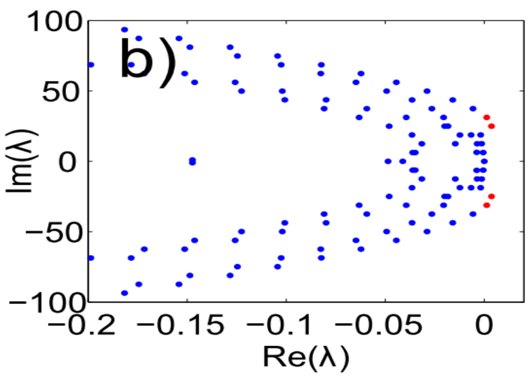

$g = 4$
$t_\pm = 0.98$
$r_\pm = 0.01$
$\varepsilon = 0.05$
$\eta = 10$
$\gamma = 250$
$\Delta = 0$
$\alpha = 2.03$

Typical parameters for semiconductor lasers

III. Longitudinal modal multistability in lasers

Bidirectional Ring laser

LSA for mode m = 2

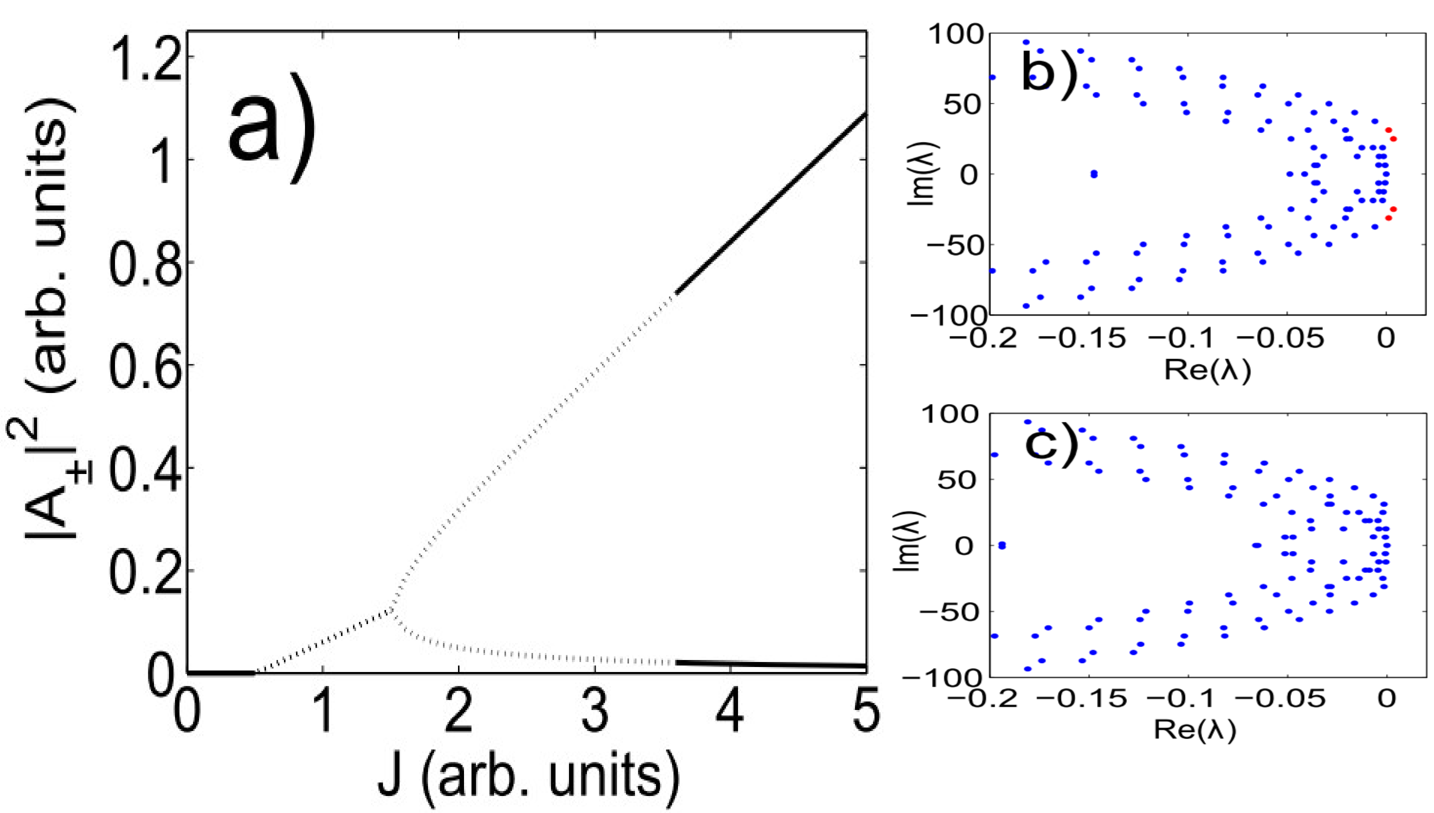

$g = 4$

$t_\pm = 0.98$

$r_\pm = 0.01$

$\varepsilon = 0.05$

$\eta = 10$

$\gamma = 250$

$\Delta = 0$

$\alpha = 2.03$

Typical parameters for semiconductor lasers

III. Longitudinal modal multistability in lasers

Uniform Field Limit (UFL)

Ring laser

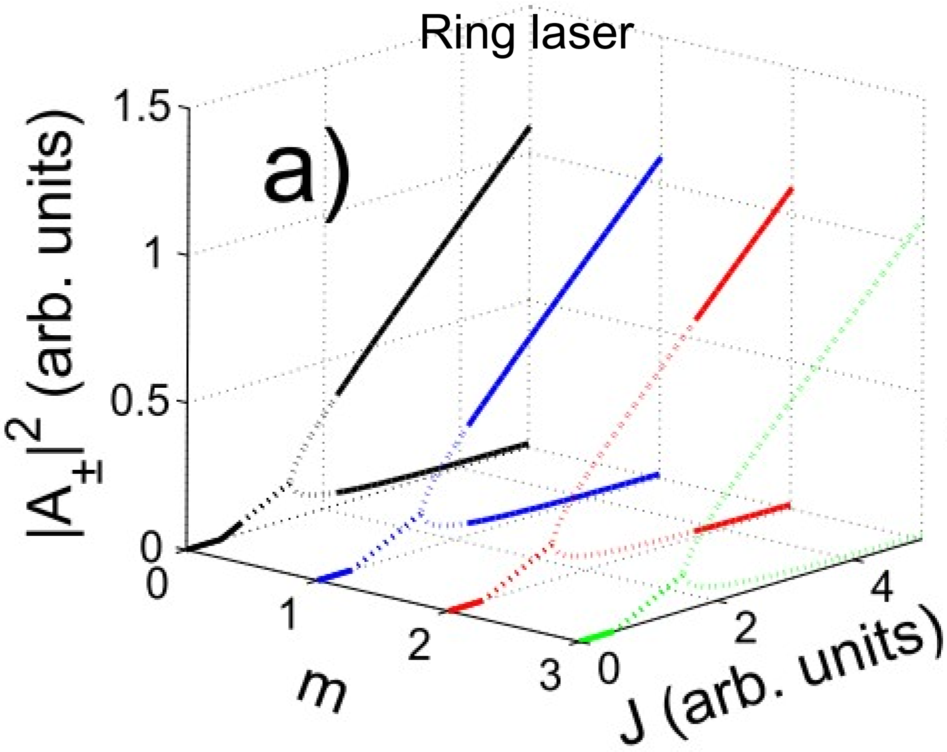

III. Longitudinal modal multistability in lasers

Fair comparison between Ring and FP lasers:

Both should work with the same degree of gain saturation, hence the pump density and the threshold pump density should be the same in both cases.

Ring: single pass on the cavity

FP: roundtrip

→ $L_{Ring} = 2 L_{FP}$

→

$g_{Ring} = 2 g_{FP}$

$\gamma_{Ring} = 2 \gamma_{FP}$

$\varepsilon_{Ring} = 2 \varepsilon_{FP}$

$\eta_{Ring} = 2 \eta_{FP}$

III. Longitudinal modal multistability in lasers

Uniform Field Limit (UFL)

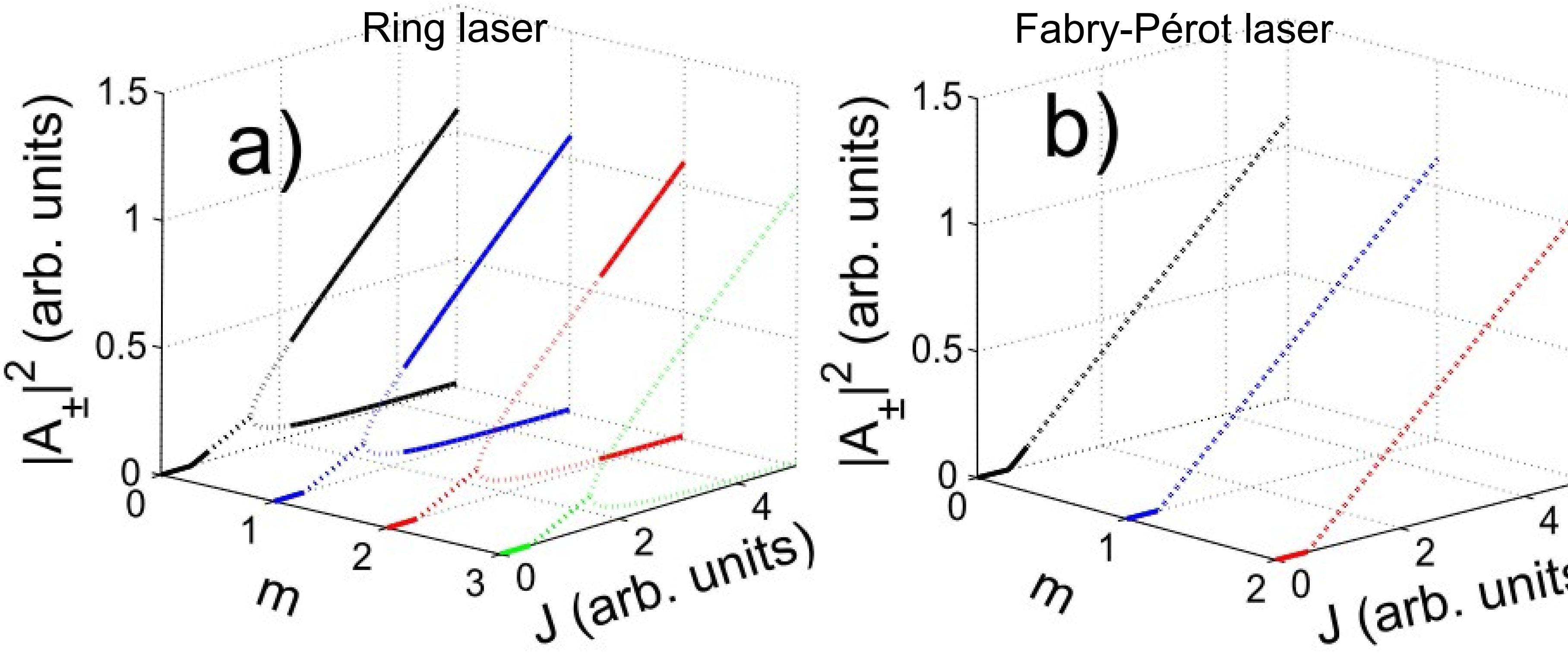

$t_\pm = 0$, $r_\pm = 0.99$, $\alpha = 1.01$

III. Longitudinal modal multistability in lasers

High losses lasers

Ring laser

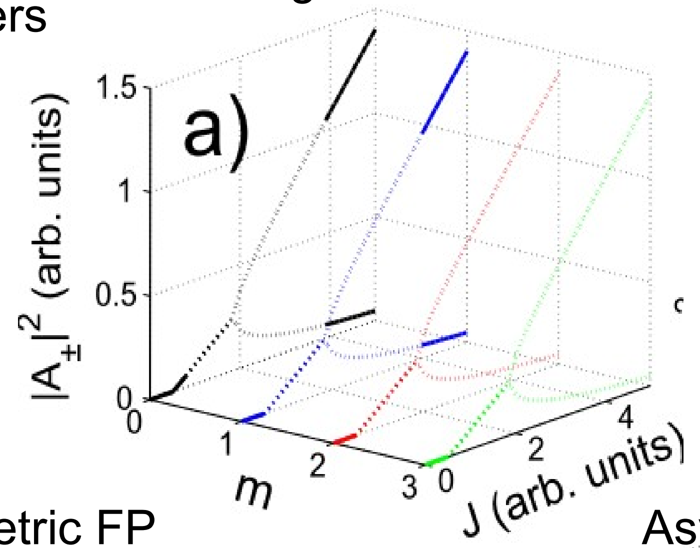

$g = 4$
$t_\pm = 0.6$
$r_\pm = 0.01$
$\varepsilon = 0.05$
$\eta = 10$
$\gamma = 250$
$\delta = 0$

$\Delta = 0$
$\alpha = 1.55$

Symmetric FP

$t_\pm = 0$
$r_\pm = 0.6$
$\alpha = 0.51$

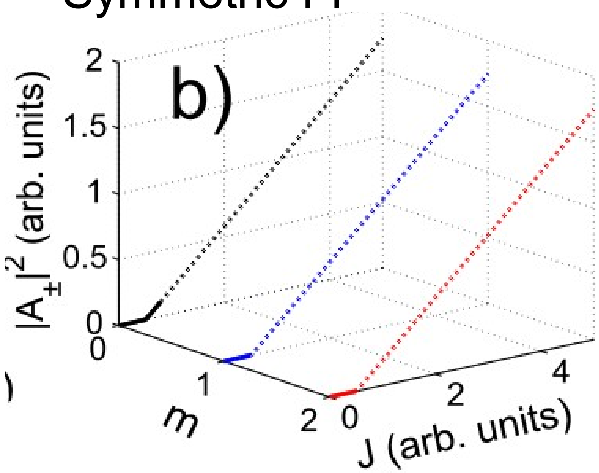

Asymmetric FP

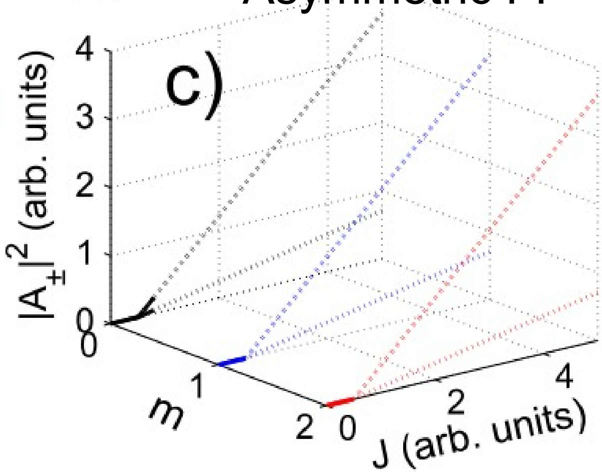

$t_\pm = 0$
$r_+ = 0.99$
$r_- = 0.2$
$\alpha = 0.21$

III. Longitudinal modal multistability in lasers

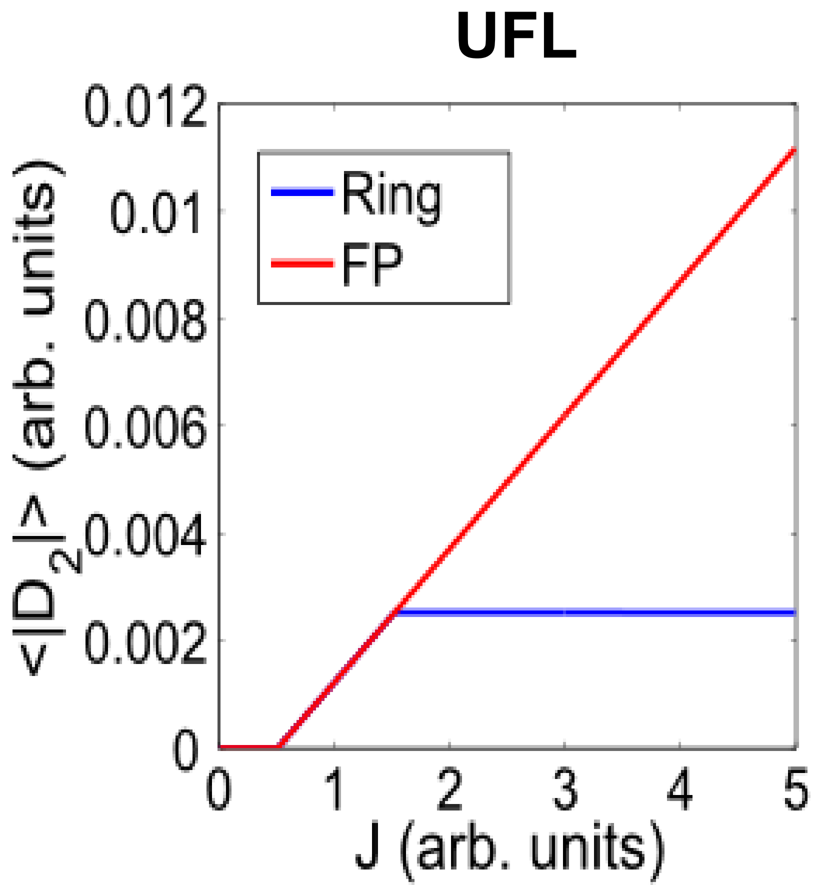

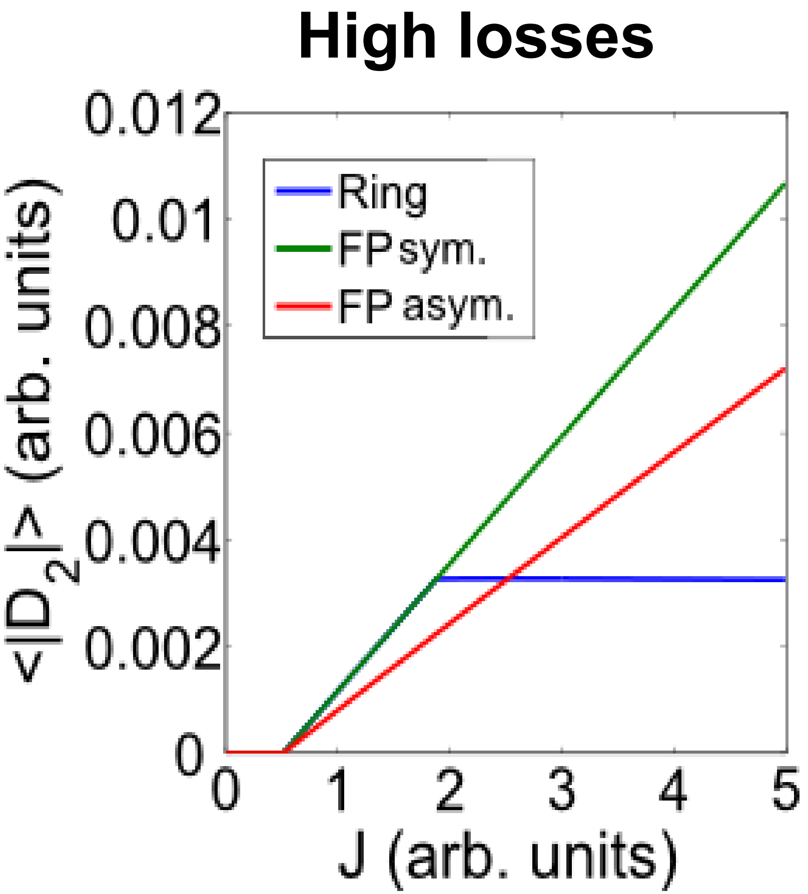

III. Longitudinal modal multistability in lasers

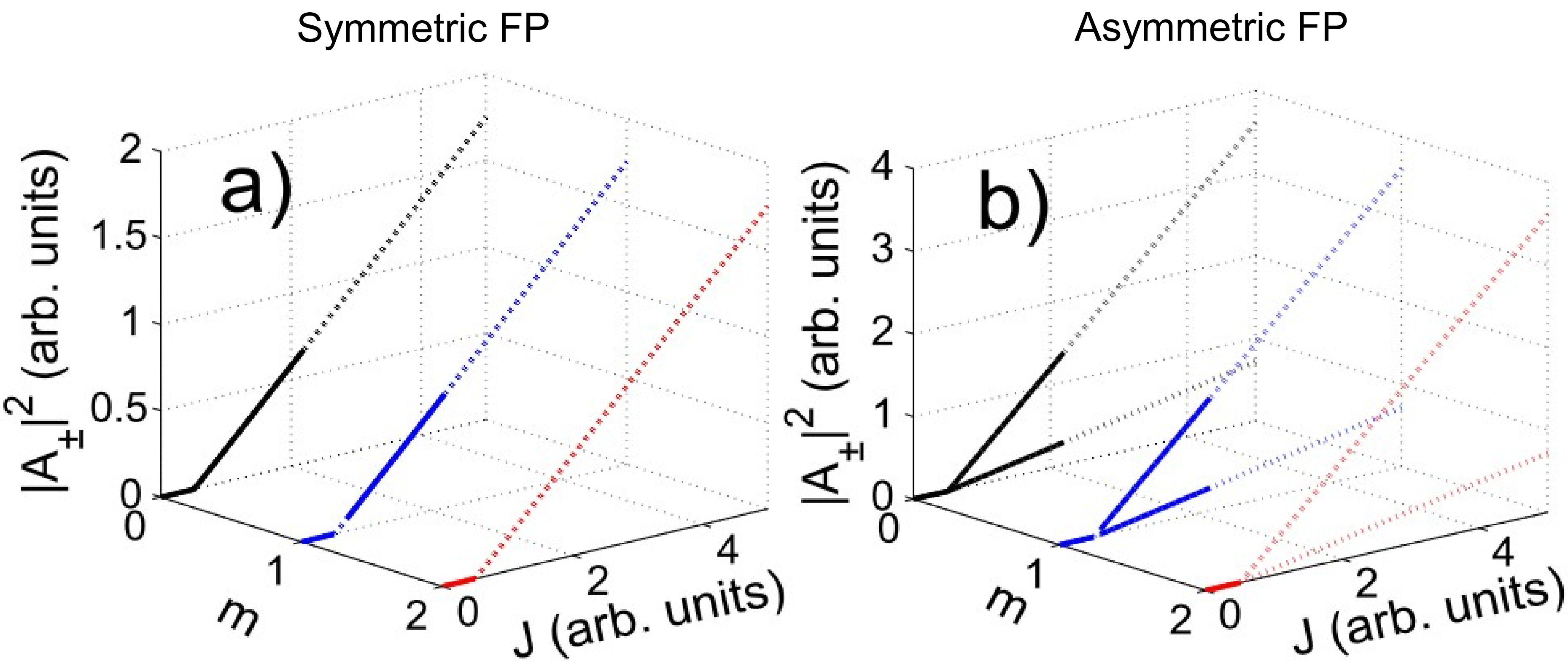

Increasing diffusion → $\eta = 10$ ⇒ Multistability in FPs

IV. Conclusions

- We theoretically discuss the impact of the cavity configuration on the possible longitudinal mode multistability in homogeneously broadened lasers based on a general form of a Travelling Wave Model.

- The LSA perfomed can be exported to other dynamical systems involving PDEs.

- Multistability is more easily reached in Ring lasers than in FP lasers and is due to the different amounts of Spatial Hole Burning in each configuration.

    - In a high quality Ring with low reflectivities, the grating terms are small, then self-saturation is smaller than cross-saturation, and multistability appears.

    - In a FP configuration the grating effects are usually important, then self-saturation is bigger than cross-saturation and multistability is not allowed. This grating effect can be reduced by increasing difussion.

Thank you for your attention!

For details:

Pérez-Serrano et al. Phys. Rev. A **81**, 043817 (2010).

Pérez-Serrano et al. Opt. Express **19**, 3284 (2011).

Financial Support:

Govern de les Illes Balears

* Numerical methodology I

Monochromatic solutions solved numerically via a multidimensional shooting method:

A guess is proposed for the modal frequency ω_0 and the fields at s = 0, $A_{\pm}(0)$

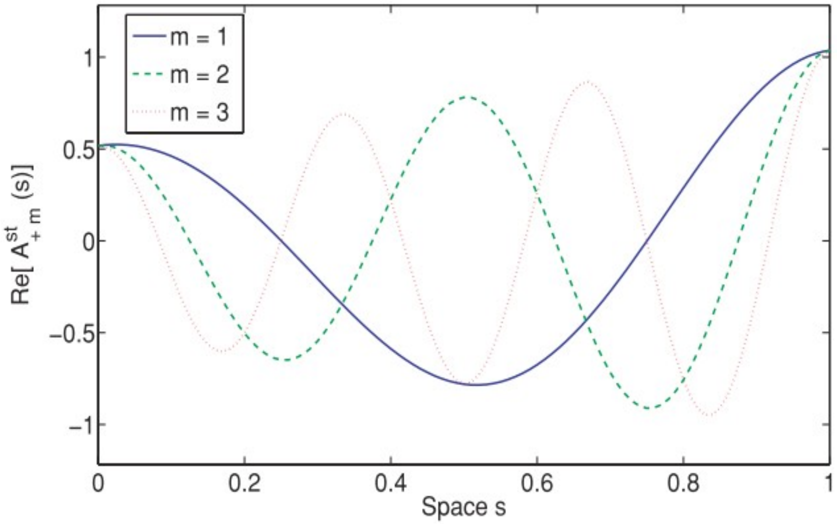

Numerical integration in space (step = 1/N)

One obtains $A_{\pm}(1)$

Verifying the boundary conditions a low dimensional Newton-Raphson computes a new guess for $A_{\pm}(0)$ and ω_0. The process is repeated until convergence.

Discretized modal profile

* Numerical methodology II (LSA)

Being **V*** a monochromatic solution, we go to the reference frame ω.

From the TWM (PDEs) we construct the evolution operator $\mathbf{U}(h,\mathbf{V}_n)$.

We use the temporal map $\mathbf{V}_{n+1} = \mathbf{U}(h,\mathbf{V}_n)$ to advance the state vector **V** a time step *h,* while verifying the Courant condition and cancelling numerical dissipation, then $\mathbf{V}^*_{n+1} = \mathbf{U}(h,\mathbf{V}^*_n) = \mathbf{V}^*_n$

We consider all possible perturbations of **V = V* + δV** finding the matrix $\mathbf{M} = \partial\mathbf{U}/\partial\mathbf{V}$
Where **M** is the linearized evolution operator.

We compute 11xN Floquet multipliers z_i of **M** $\lambda_i = h^{-1} \ln z_i$

* e.g. N = 256, standard PC using C++ routine based on *Octave*

Monochromatic solution → 1 s
Generating **M** → 10 s
Diagonalizing with QR decomposition → 60 s